Anatomy of noise in quantitative biological Raman spectroscopy

Janusz M. Smulko[*1,2], Narahara Chari Dingari[1], Jaqueline S. Soares[1,3] & Ishan Barman[4]

[1]G. R. Harrison Spectroscopy Laboratory, Massachusetts Institute of Technology, Cambridge, Massachusetts 02139, USA

[2]Gdansk University of Technology, Faculty of Electronics, Telecommunications and Informatics, G. Narutowicza 11/12, 80-233 Gdansk, Poland

[3]Departamento de Fisica, Universidade Federal de Ouro Preto, Ouro Preto, MG 35400-000, Brazil

[4]Department of Mechanical Engineering, Johns Hopkins University, Baltimore, Maryland 21218, USA

[*]Author for correspondence:

E-mail: jsmulko@eti.pg.gda.pl

Abstract

Raman spectroscopy is a fundamental form of molecular spectroscopy that is widely used to investigate structures and properties of molecules from their vibrational transitions. It relies on inelastic scattering of monochromatic laser light irradiating the specimen. The scattered light after appropriate filtering is dispersed onto a detector to determine the shift from the excitation wavelength, which appears in the form of characteristic spectral patterns. The technique can investigate biological samples and provide real-time diagnosis of diseases. However, despite its intrinsic advantages of specificity and minimal perturbation, the Raman scattered light is typically very weak and limits applications of Raman spectroscopy due to measurement (im)precision, driven by inherent noise in the acquired spectra. In this article, we review the principal noise sources that impact quantitative biological Raman spectroscopy. Further, we discuss how such noise effects can be reduced by innovative changes in the constructed Raman system and appropriate signal processing methods.

Key Terms

Thermal noise: Johnson–Nyquist electronic noise caused by thermal movements of the charge carriers (e.g., in the trans-impedance amplifier) independent of any applied voltage. Power spectral density of thermal noise is constant and has a Gaussian amplitude distribution at finite bandwidth.

Power spectral density: Function that describes how power of the signal is distributed over the different frequencies.

Flicker noise (1/f noise): Type of electronic noise with a power spectral density that depends on frequency as $1/f^{a}$, where the parameter *a* is usually equal to 1 or greater.

Shot noise: Type of electronic noise, which results from the discrete nature of the measured quantity. Shot noise is observed in current flow due to discrete number of electrons. For the subject under consideration, shot noise is associated with the particle nature of light (stream of photons).

Dark current: The (relatively small) random current flowing through the photosensitive device when no photons are entering the device. The current is due to generated electrons and holes in

semiconductor crystallographic defects within its depletion region. Intensity of dark current depends on temperature of the photosensitive device.

Signal-to-noise ratio (SNR): A measure that compares the signal intensity to the level of background noise present at measurements. Usually, logarithmic scale of dB is applied. This measure is extensively used to characterize the measurement capability of a wide variety of electronic, physical and photonic signals and devices.

Introduction

Raman spectroscopy is a widely used spectroscopic technique to observe vibrational, rotation, and other low-frequency modes of the investigated specimen. The method utilizes laser light to irradiate the sample, which excites the molecule(s) of interest to virtual energy states (Figure 1). In classical terms, Raman-active vibrational transitions can be viewed as altering the polarizability of the molecule. From the quantum mechanics perspective, the molecule(s) return from the virtual energy states to the ground electronic state, but different vibrational states – during which process of relaxation, the molecule(s) emits a photon. The difference in energy between the original state and this new state leads to a shift in the scattered photon's frequency away from the excitation wavelength.

If the final vibrational state of the molecule is more energetic than the initial state, then the Raman-scattered photon will be shifted to a lower frequency (“red-shifted”) in order for the total energy of the system to be conserved. This shift in frequency is designated as a Stokes shift. On the other hand, if the final vibrational state is less energetic than the initial state, then the scattered photon will be shifted to a higher frequency (“blue-shifted”), and this is commonly designated as an anti-Stokes shift. This shift appears in the form of characteristic spectral patterns or, Raman fingerprints.

The Raman-scattered light is collected by suitable lenses or fibers and is sent through a monochromator or a dispersion spectrometer before recording on the detector (such as a charge coupled device, CCD, or complementary metal-oxide-semiconductor, CMOS, chip). It is important to reject wavelengths close to the laser line that are present due to the Rayleigh (elastic) scattering contribution. This component has to be removed because it is relatively very intense. Contemporary Raman systems employ specialized notch or edge filters for such rejection.

Evidently, Raman scattering is an inelastic scattering process because of the energy transfer between the photons and the molecules during their interaction. The spontaneous Raman effect should not be confused with absorption and/or fluorescence where the molecule is excited to a discrete (not virtual) energy level. Since vibrational information is specific to the chemical bonds and can characterize the specimen functional groups and related components, Raman spectroscopy is widely used in chemistry and biology [1-9]. In particular, this has meant that biological specimens (cells, tissues and even organs) can be characterized by Raman spectroscopy noninvasively by exposing to laser radiation of limited optical power. Recent years have, further, seen the advance and popularization of this method primarily due to the considerable improvements in laser technology, excitation-collection optics, CCD detectors and advances in signal processing [10-14].

Despite its inherent advantages in chemical specificity and lack of sample preparation or perturbation requirements, spontaneous Raman spectroscopy suffers from weak signals in comparison to other chemical fingerprinting modalities including fluorescence, absorption and

reflectance spectroscopy. For example, the spontaneous Raman signal is at least a few orders of magnitude weaker than the Rayleigh scattered light, thus necessitating optical filtering to avoid saturation of the detector. The ability to extract information about composition of the investigated specimen is usually limited by intensity of noise, which can overwhelm the main signal [13-19]. Notably, one of the central hurdles in attaining robust quantitative Raman measurements is the presence of a varying luminescence (fluorescence) background. The substantially greater intensity of the tissue fluorescence frequently limits analysis to strong Raman bands only, as evidenced by the intensity comparison provided in Fig. 2. The associated noise contribution, which may have intensities similar to that of the Raman signal depending on the signal acquisition times, further compromise the capability of the spectroscopic technique.

Amplification of Raman scattering light (e.g., by surface enhanced Raman spectroscopy [20]) to increase signal and reduce noise have limited applications because such conditions cannot be implemented in each case. Also, the amplification effect varies between the measurements resulting in severe reproducibility constraints. Further, while the Raman scattering signal at higher excitation powers would be enhanced, there are critical limitations to the maximum power that can be employed emanating from safety concerns on the investigated specimen. Notably, it would also increase the fluorescence background that is the source of specific noise components (including pixel-to-pixel detector noise and shot noise), as detailed later in this article.

While technological developments within the last decade have helped to enhance the relevant signal-to-noise ratio (SNR), this issue still remains a major impediment in a variety of Raman spectroscopy applications. In order to ensure low noise in the acquired spectra, one requires customized, expensive and often bulky instrumentation, which limits its usage. Therefore, it is imperative that appropriate noise sources are identified and reduced as much as possible to assure high SNR value – without requiring to resort to unnecessary complexity in terms of hardware and software incorporation.

Measures and principles of noise characterization

The SNR parameter is often estimated separately for each peak of the Raman spectrum because optical characteristic of the spectrometer-detector combination can influence the intensity of noise at various Raman shifts (Figure 3). Its value at a specific Raman shift equals the averaged peak height μ_P divided by the standard deviation σ_P of that peak: $SNR = \mu_P/\sigma_P$. The definition determines how additive noise influences each separate peak of the measured spectra. The parameter SNR can be established by numerous measurements of the Raman spectra and estimation of the average peak value and its standard deviation at each Raman shift separately. The presented definition is very straightforward but there are several instances in the literature where the SNR, in fact, is estimated using standard deviation σ_S of the whole Raman spectrum instead of σ_P, estimated at a given Raman shift. Usually σ_S and σ_P are of different value and such computation may therefore provide inaccurate estimates.

The SNR, clearly, is driven by the intensity of noise sources during the acquisition process, some of which may be amenable to reduction. In other words, technological advances can reduce only selected noise sources. Therefore, inherent noise sources of the Raman system have to be identified to establish, which of them can be reduced at limited costs or acquisition time. Longer averaging, for example, results in gain of Raman signal by increasing number of the acquired electrons and improving SNR when the limiting noise source is “white” (e.g., shot noise and thermal noise having flat power

spectrum independent from frequency). On the other hand, when 1/f noise is the limiting contribution especially at low frequency range, there exists an optimal acquisition time in order to obtain the highest SNR value. In such circumstances, prolonged acquisition would actually decrease the resultant SNR. Another technique that can reduce noise in the measured spectrum utilizes synchronous detection, when the laser power is modulated using selected frequency and the Raman spectrum is acquired to detect the part, which is synchronous to the modulated laser beam. A certain measure of de-noising can also be performed subsequent to data acquisition by modeling the peaks and reducing random component by additional filtering. At least a few independent algorithms can be successively applied.

Notably while the weak Raman effect is an impediment for molecular identifications and scientific investigations, problems of biomedical interest frequently involve complex mixtures of stochastically varying compositions and spatial distributions of analytes contributing to the acquired spectra [10, 14]. Thus, the challenge here is further compounded by the need to quantitatively determine chemical markers that facilitate rapid detection of species (such as protein conformations, strains of bacteria) or suggest changes in function in biological tissue (e.g. benign versus malignant tissue). The overarching challenge is that the combined measurement and analysis has to be rapid while also being robust with respect to stochastic variance.

In the following sections, we elaborate on the noise sources that hinder such quantification and classification capabilities and the origins of the noise contributions. We also review emerging methods that have been presented to address some of these noise sources and how they influence our capability to quantify analytes based on Raman spectra. We discuss the applicability, advantages and drawbacks of each of these techniques and assist the reader not only acquire new insights into the techniques themselves but also gain an understating of the underlying ideas and principles.

Noise sources

In this section, the principal, independent sources of noise that manifest themselves in Raman spectra acquired from biological samples are considered. When the sources are independent (i.e. uncorrelated), their intensity (determined by the variance σ^2) can be calculated by summing up variances of all considered sources. Usually, for such computation, the noise sources are limited to the most important ones and identified by their different generation mechanisms [14]:

$$\sigma^2 = \sigma_x^2 + \sigma_b^2 + \sigma_d^2 + \sigma_f^2 + \sigma_r^2 \tag{1}$$

where σ_x is a standard deviation of signal *x* due to uncertainty in counting statistics of the signal photons, σ_b is a standard deviation of background fluctuations, σ_d is a standard deviation of detector dark current, σ_f is a standard deviation of flicker noise and σ_r is a standard deviation of readout noise. These noise sources result from the process of Raman spectra measurement and stream nature of the collected photons.

Photons stream or resulting electron stream observed as the voltage drop (Figure 4) exhibits shot noise because of its discrete nature. Standard deviation of any signal being a stream of discrete events is proportional to the square root of the signal (Poisson statistics) and is a natural limit of such signal measurement uncertainty, even when other noise sources can be neglected. Thus, in a case that only shot noise of electrons is considered the SNR depends on signal *x* intensity as:

$$SNR = x/\sigma_x = x/x^{1/2} = x^{1/2}. \tag{2}$$

When shot noise predominates noise in Raman spectra the SNR can be improved by increasing averaging time t. The signal $x = x_o t$ increases proportionally with time t (number of the collected electrons) and therefore SNR can be equated to $(x_o t)^{1/2}$.

The next considered noise source is caused by background noise, which is a combined effect of the variations in the excitation source and spectrometer-detector combination. The latter encompasses the pixel-to-pixel variations that can often be substantive especially when acquisition times are relatively large. The background noise can be reduced by changing laser wavelength to the near infrared (NIR) region to diminish fluorescence or by applying mathematical algorithms to remove background (especially the pixel-to-pixel) variations [21-26].

One of the most important noise sources in Raman spectroscopy is generated within the applied detectors and is known as dark noise. This is a random stream of electrons caused mainly by thermal generation of electrons, independent of the intensity of the collected light. Put another way, dark noise originates from the statistical variation in the number of electrons thermally generated within the silicon structure of the CCD, which is independent of photon-induced signal, but highly dependent on the device temperature. Similar to shot noise, dark noise follows a Poisson relationship and is equal to the square root of the number of thermal electrons generated within the image exposure time. This noise component, though, can be strongly reduced when the employed detector is cooled (Figure 5). Intensity of dark current can vary for various detectors from a few hundreds of e^- /s (electrons per second) to negligible values when the detector is significantly cooled.

Typically, an additional control unit has to be utilized to keep the detector at stable temperature. The control unit can itself generate fluctuations at low frequency range, when the detector temperature is stabilized within the acceptable range. Power spectral density of such fluctuations depends on frequency as $1/f^a$ where the parameter a is usually close to unity and is called 1/f noise [27-29]. Another source of 1/f noise in the Raman spectrometer are caused by power fluctuations of the emitted laser beam, mainly due to slow temperature variation of the laser [30]. These components are represented by standard deviations σ_f and can overwhelm other noise sources, at least in the low frequency domain.

Finally, the readout noise, represented by standard deviation σ_r in Eq. (1), is a combination of system noise components intrinsic to the process of transforming the CCD charge carriers into a quantitative voltage signal, and the subsequent processing and analog-to-digital conversion. This process requires sampling of the voltage drop across the resistance R (Figure 4) and some necessary amplification to adjust the voltage drop to the dynamic range of the applied analog-to-digital converter. The major contribution to readout noise usually arises from the on-chip preamplifier, and this noise is added uniformly to every image pixel. The readout noise depends on quality of the Raman system and can be reduced to intensity levels much lower than other mentioned noise sources. Additionally, intensity of the readout noise does not depend on time. Thus, lengthening averaging time can reduce influence of these noise components and assure high SNR ratio.

Methods of noise reduction

Of the mentioned noise sources that hinder the recording of the intrinsic Raman signal, only a few of the contributions can be appropriately reduced by different methods including hardware

modifications. There is a natural limit of noise which cannot be reduced but its influence on the quality of the acquired Raman spectra can be reduced mainly by longer averaging time [21]. As mentioned earlier the SNR increases with time as SNR = $(x_o t)^{1/2}$ when noise in Raman spectra is dominated by shot noise. This principle is equally valid for the dark current noise. When the readout noise is dominant, the SNR will increase even faster with averaging time than for shot noise components. Thus, longer averaging time can increase SNR to the requisite values with increase in the acquisition time window.

However, this holds true only when the white noise component is present in the Raman spectra. In sharp contrast, for flicker ($1/f^a$) noise (which due to its structure tends to dominate in the low frequency region), further increase of acquisition time can result even in reduction of resultant SNR. This issue was considered in detail in literature [22]. It was determined that for 1/f noise (a = 1) increasing averaging time improves SNR up to a certain threshold level only. The SNR saturates after a period of time, which depends on the relative intensities of 1/f noise and white noise components. It is also evident that the optimal averaging time become shorter and the maximum possible SNR reduces when the parameter a increases. Further, in numerous biological applications the averaging time cannot be too long not because of the 1/f noise component issue but because of the potential changes in the specimen under investigation. Thus, other methods have to be applied to address the respective noise components.

The dark current noise predominates often in commercial Raman spectrometers in relation to the other noise sources and the simplest method of improving the SNR, under such circumstances, is to cool down the CCD sensor (Figure 5). Typically, the CCD sensor is of area about a few tens of mm^2 that has to be cooled to reduce dark noise. Thermoelectric cooling is usually employed in portable Raman spectrometers because such unit can be easily controlled by an electronic circuit and, importantly, because it does not require incorporation of bulky elements of high energy consumption [23]. For example, the CCD detector is cooled down by applying a Peltier cooler which comprises of two metal plates sandwiched between which is a semi-conducting material. This device acts as a heat pump when the current flows between the metal plates. It pulls heat from the CCD detector onto the Peltier cooling device, and subsequently dissipates the heat via radiating fins. The CCD detector can be kept cooler anywhere from -30^{o}C to -70^{o}C below the ambient temperature. In some cases, CCD detectors employ a two-stage Peltier cooler to improve the effectiveness of the device. Such a thermoelectric cooling unit, however, stabilizes temperature within some limited range only and may cause slow drifts that adversely affect the noise level as well. Better stability is achieved when the CCD chip and a multi-stage Peltier cooler are built into a welded chamber vacuumed and hermetically sealed to retain a high degree of vacuum and assure more stable cooling performance. Lower and more stable temperatures are obtained in laboratory systems when the CCD detector is cooled by liquid-nitrogen. In addition, it provides better temperature stability – although its application in extensive clinical applications is limited due to necessity for regular refilling of liquid nitrogen and its generally unwieldy nature.

Another important source of noise is the random but fixed variations in pixel-to-pixel response on the CCD might actually be more dominant than shot noise. This is especially true when high signal levels can be achieved and exposure times can be increased without any significant downside, such as when chemical mixtures and powder samples are tested. In such cases, the nearly 1% pixel-to-pixel variations may contribute to a larger portion of the overall uncertainty as compared to the shot noise. An elegant, and relatively underappreciated, method is to employ difference spectroscopy between two frames. As has been discussed by Bell and co-workers [31-33], performing shifted excitation Raman difference spectroscopy (SERDS) or shifted subtracted Raman difference spectroscopy (SSRS) by tuning the excitation wavelength or diffraction grating, respectively, one can concomitantly perform

rejection of the fluorescence background and remove the fixed pattern noise from the acquired spectra.

Alternately, investigators have also employed the principle of phase-sensitive detection (lock-in amplifier) for noise reduction in the acquires Raman spectra. In this method, one modulates the optical power of the laser beam at a given frequency and filters out within the measured Raman spectra the component having the same frequency as the modulation of the laser beam [24]. Such method has been observed to reduce noise components caused by dark noise of the CCD detector, readout and 1/f noise or induced by external light sources that are uncorrelated with the important Raman photons. Technically, the process requires multiplication (mixing) of the measured Raman spectrum and the reference signal that is used to modulate the laser beam. The product of multiplication is proportional to the Raman scattering signal and has to be averaged to filter out the stochastic components. Nevertheless, the lock-in amplification method has specific limitations especially when employed for investigation of biological samples, as it requires long averaging time and does not reduce fluorescence.

Finally, an intriguing approach that has come into prominence of late in this area is spatially offset Raman spectroscopy (SORS) [25,26]. SORS requires the physical positioning of the excitation source and detector to be spatially offset by pre-determined distances. In particular, for a fiber probe based system, the excitation and collection fibers in SORS are often separated by several mm, as opposed to the conventional fiber probe where all the fibers are grouped together to enhance volume fraction of photon collection. This allows probing at greater depths than is traditionally achievable using conventional illumination and collection systems. In essence, the SORS geometry allows the SNR of the analyte(s) of interest to be maximized by selecting appropriate spatial offset between the collection areas [26]. We expect that the convenience and ease of use of this method will allow its widespread application in deep tissue measurements highlighting new ways in which the relevant noise sources (in this case, the signal from the non-analyte specific region of the tissue) can be suppressed.

Spectral processing

Despite the advances in the spectroscopic hardware and emerging concepts of robust measurement, the acquired Raman spectra (especially in biological samples) reveal substantive “uncertainty”, emanating both from the inherent noise of the measurement system and the stochastic nature of the Raman scattered light. In other words, further noise reduction beyond a threshold level can often be impractical due to prohibitive costs or unacceptable measurement conditions, such as excessively long exposure time or too intense irradiation of the biological tissues. Thus, processing methods subsequent to spectral recording have to be designed and employed to reduce noise and/or suppress its effect in the robust mapping between spectroscopic measurements and biomarker information. Specifically, multivariate chemometric techniques have been widely investigated, as they are capable of extracting information otherwise hidden from human examination. Indeed, the richness and availability of myriad data enable vibrational spectroscopists to both use methods from and actively contribute to the development of chemometric techniques. Given the scope of the current review, we confine ourselves to a selection of numerical algorithms that seek to improve data quality, principally the signal-to-noise ratio. The other category of chemometric applications in spectroscopy deals with the classification of information from the data (both supervised and unsupervised methods), the prediction of biomarker content based on acquired datasets and the visualization of the resultant information.

An important avenue for active research in this direction is the selection of suitable features (or Raman information) that allow the elimination of uninformative and spurious regions of the spectra from the developed models. In a recent study, our laboratory has observed that reduction of the wavelengths probed by a factor of 10 did not provide a substantive hurdle to developing a calibration model for estimation of blood glucose levels [34,35]. Additionally, selection of limited wavelength subsets may provide new impetus to the development of tunable detection filter-based serial Raman acquisition systems. These systems would greatly alleviate the large spatial footprint drawback of standard Raman systems based on dispersive spectrometers but suffer from longer acquisition time requirements. By employing only a fraction of the total set of wavelengths, one can envision a significant reduction in the acquisition time because of the serial sampling nature of such systems.

Existing methods of addressing some of the pre-dominant issues with biological Raman spectra include the use of smoothing algorithms (since signals are generally concentrated in lower frequencies while noise is spread across the spectrum) and background correction to compensate for the slowly varying luminescence background [36]. For example, Fig. 6 shows raw Raman spectra recorded from a strongly scattering sample and also its counterpart post smoothing using the widely used Savitzky-Golay filtering algorithm. The background is typically suppressed by derivative processing or least squares polynomial subtraction methods [37]. However, we are generally less enthused about the application of these methods for purposes of classification or quantification, as these techniques may often introduce spectral artifacts. As alluded to above, much more efficient methods of fluorescence background removal would be those based on continuous shift of the excitation wavelength [38-41]. These methods are based on the differential shift response of the Raman and fluorescence signals to the shift in excitation wavelength, and offer a promising solution that is not limited by photon collection problems, unlike time-gating approaches. Here, the Raman peaks can be de-convolved from the subtracted signal by taking into account the amplitude and the modulation rate of the excitation wavelength [39].

It is worth noting that some studies have attributed the background observed in Raman spectra from biological samples to sources other than fluorescence from endogenous chromophores. For example, Bonnier and co-workers have suggested the possibility that the background may be caused by scattering phenomena [40]. It has previously been observed that the broad background appears to shift in the same direction as the excitation wavelength when a tunable laser is employed indicating Raman-like scattering origin [41]. Such non-specific scattering baseline could be ascribed to the presence of intermolecular effects that depend on the laser exposure, temperature and ligand exchange among other things [42]. To potentially alleviate the background arising from such sources, immersion of the biological specimen in aqueous solution has been specifically proposed to improve the refractive index matching between the tissue and surrounding media [40]. Additionally, water solution is necessary to keep the investigated objects alive and helps to enhance their photostability. Moreover, it improves heat flow of the irradiated biological membranes and reduces chances of eventual tissue overheating due to prolonged irradiation.

There are other interferences present in Raman spectra in addition to the aforementioned noise components and (fluorescence and broad-band) background. The acquired Raman spectra exhibit often very narrow spikes caused by cosmic irradiation [45]. Cosmic ray interference can be reduced by applying an algorithm that estimates a width of the identified spike and removes it by replacing the spike value with an average estimate based on the intensity of the neighboring pixels. The underlying assumption is that the width of the cosmic ray is smaller than a pre-defined threshold and cannot be considered as a Raman feature of interest. Analogous noise can be observed when some

of the pixels in the applied optical sensor record extreme values only (maximum or minimum). This type of noise is known as salt-and-pepper noise in imaging literature and is also interchangeably referred to as the “hot pixel” issue in spectroscopy [46]. It can be problematic when the Raman spectra are used to present images of the tissues to identify demarcating borders of the selected regions, such as for intra-operative margin assessment of cancerous tissue. The median filter or its modified versions are commonly used to remove such high frequency impulse noise [47].

It is important to understand that fundamentally, the process of any noise rejection involves recognizing some characteristic of noise that is distinct from that of the signal, transforming the data such that the relevant measures of the property are highlighted, suppressing the noise-related property values and inverse transforming the data to recover high SNR data. As discussed elsewhere in the literature [48], the transformation may involve simple smoothing, determining correlations using point-wise or multivariate means or statistical reconstruction. For practical purposes, there is no single cure-all that can be applied universally. Instead, the quantity of available data frequently dictates the optimal method. A particularly interesting approach in this regard is the use of multivariate covariance method when large numbers of spectra are available. Briefly, the approach comprises of eigenvalue decomposition of the spectra employing a forward transform, such as by using principal components analysis (PCA) to transform the dataset into a few orthogonal components [49,50]. After choosing the principal components that exhibit sufficient SNR, the chosen data are inverse-transformed to recreate the original data set with substantially reduced noise content. Such transform techniques for noise reduction exploit the property that noise is uncorrelated whereas the characteristic spectral patterns show a much higher degree of correlation. In other words, in the transform domain, the signal becomes largely confined to the first few eigenvalues while the noise content is distributed across a significantly larger number of principal components. It is the signal to noise content of a particular principal component that influences the decision of its inclusion when the inverse transform operation is performed. Despite the intrinsic attraction for such de-noising procedures, it is pertinent to note that the results from any of the above methods must be validated rigorously, especially in a prospective manner, if the method is to be routinely employed.

Finally, processing of the recorded Raman spectra has to be undertaken in biomedical applications with the goal of predicting concentrations of biomarkers in complex specimen or classifying their function within the context of varied patho-physiological states. This means that the pre-processed (and potentially noise suppressed) spectra have to be used in conjunction with the reference information content (such as concentrations, histo-pathological classification) to develop a model that can prospectively provide the same information in unknown samples [51-55]. The developed chemometric algorithms should identify effectively the constituents of the investigated specimen and should be robust against noise and interferences present in the recorded Raman spectra. Additionally, they should not require intense computing in order to ensure they can be incorporated in inexpensive and portable systems, although the constraint in this direction is rapidly decreasing due to the explosion of computing power in recent years.

It should be emphasized that there are no generic guidelines when a particular method for noise reduction (hardware implementation or numerical processing) would be optimal for the application under consideration. Indeed, the responsibility lies with the investigator to explore different methods and determine the potential for improvement of the overall signal quality. For example, detector cooling improves the SNR of spectral datasets particularly for NIR applications. However, once the system is shot-noise limited, such cooling could even adversely affect as the quantum efficiency of sensor chips may reduce at very low temperatures. Similarly, spectral smoothing, though extensively used, often results in some unavoidable spectral lines’ deformation,

compromising the ability to accurately detect and quantitate the bioanalytes. The spectroscopist must be aware, therefore, that the best option for accurate quantitative analysis is to simply acquire higher SNR data, if at all feasible.

Future perspective

The requirements for quantitative Raman spectroscopic measurements are continuously increasing due to the growing number of applications that demand high fidelity and sensitivity data. It is in this context that the noise characterization of the Raman measurements (and investigation of the response of the developed model to noise) is critically important. Such investigations are imperative for successful clinical translation as the confidence in the measurement of a specific diagnostic parameter can alter the course of disease management, with ramifications to the health of the patient. The response of the prediction algorithm to noise sources in the data set could critically affect the diagnostic value of the data. It may also influence the evaluation of one type of protocol against another and suggest the use of modified experimental conditions to boost results. A fundamental understanding of the noise sources and the possibility (or lack thereof) of reducing them are key to elucidating the true scientific content of the data structure and are key to enabling accurate, fast, and robust information extraction from the acquired spectral datasets. Clearly, this requires an understanding of the interplay between the hardware and software elements. We envision that, in the near future, fundamental biochemical insights and *a priori* knowledge will also be integrated with system design and strategies for data processing to guide the information extraction and algorithm development process. Future investigations will need to focus on the development of such integrative approaches especially to address clinical specimens, where the signals of interest are often very low in comparison with the background.

Executive summary

- Intense noise is a significant challenge in quantitative biological spectroscopic measurements and requires detailed consideration. (**Measures and principles of noise characterization**)
- Inherent noise can be reduced only to a certain extent due to physical limitations and even then such reduction strategies may necessitate impractical approaches, prohibitive costs, loss of functionality. (**Noise sources**)
- Synchronous detection and longer averaging time of the acquired spectra reduces noise in the recorded spectra but can be accepted only in some biological applications. (**Methods of noise reduction**)
- Spectral pre-processing and optimized classification and regression algorithms can reduce the sensitivity to noise levels. We strongly believe that new proposals in this area will emerge as the primary thrust for improving overall measurement capability and therefore in further popularization of Raman spectroscopy. (**Spectral processing**)

References

1. Dingari N, Horowitz G, Kang J, Dasari R, Barman I. Raman Spectroscopy Provides a Powerful Diagnostic Tool for Accurate Determination of Albumin Glycation. *Plos One*, 7(2) (2012).

2. Gonzalez F, Alda J, Moreno-Cruz B *et al.* Use of Raman spectroscopy for the early detection of filaggrin-related atopic dermatitis. *Skin Research and Technology*, 17(1), 45-50 (2011).
3. Kang J, Lue N, Kong C *et al.* Combined confocal Raman and quantitative phase microscopy system for biomedical diagnosis. *Biomedical Optics Express*, 2(9), 2484-2492 (2011).
4. Filik J, Stone N. Analysis of human tear fluid by Raman spectroscopy. *Analytica Chimica Acta*, 616(2), 177-184 (2008).
5. Huang W, Pan J, Chen R *et al.* Measurement of Nasopharyngeal Carcinoma Tissue ex vivo by Raman Spectroscopy. *Spectroscopy and Spectral Analysis*, 29(5), 1304-1307 (2009).
6. Barman I, Dingari NC, Saha A *et al.* Application of Raman spectroscopy to identify microcalcifications and underlying breast lesions at stereotactic core needle biopsies. *Cancer Research*, 73, 3206-3215 (2013).
7. Nakagawa N, Matsumoto M, Sakai S. In vivo measurement of the water content in the dermis by confocal Raman spectroscopy. *Skin Research and Technology*, 16(2), 137-141 (2010).
8. Barman I, Singh G, Dasari R, Feld M. Turbidity-Corrected Raman Spectroscopy for Blood Analyte Detection. *Analytical Chemistry*, 81(11), 4233-4240 (2009).
9. Kumar R, Singh GP, Barman I, Dingari NC, Nabi G. A facile and real-time spectroscopic method for biofluid analysis in point-of-care diagnostics. *Bioanalysis*, 5(15), 1853-1861, (2013).
10. Zeng H, Zhao J, Short M *et al.* Raman spectroscopy for in vivo tissue analysis and diagnosis, from instrument development to clinical applications. *Journal of Innovative Optical Health Sciences*, 1(1), 95-106 (2008).
11. Shao Y, Qu J, He Y, Schweitzer D, Fitzmaurice M. In vivo measurement of the carotenoid level using portable resonance Raman spectroscopy - art. no. 662817. *Diagnostic Optical Spectroscopy in Biomedicine Iv*, 6628, 62817-62817 (2007).
12. Kong CR, Barman I, Dingari NC *et al.* A novel non-imaging optics based Raman spectroscopy device for disease diagnosis. *AIP Advances*, 1, 032175 (2011).
13. Ramirez-Elias M, Alda J, Gonzalez F. Noise and Artifact Characterization of in Vivo Raman Spectroscopy Skin Measurements. *Applied Spectroscopy*, 66(6), 650-655 (2012).
14. McCreery Richard L. Raman spectroscopy for chemical analysis. Vol. 225. Wiley. 49-71 (2005).

** Comprehensive review of selected noise phenomena in Raman spectrometers

15. Van de Sompel D, Garai E, Zavaleta C *et al.* Comparison of Gaussian and Poisson Noise Models in a Hybrid Reference Spectrum and Principal Component Analysis Algorithm for Raman Spectroscopy. *Single Molecule Spectroscopy and Superresolution Imaging Vi*, 8590 (2013).
16. Barman I, Kong CR, Singh GP, Dasari RR. Effect of photobleaching on calibration model development in biological Raman spectroscopy. *Journal of Biomedical Optics*, 16(1), 011004 (2011).
17. Quintero L, Matthaus C, Hunt S *et al.* Denoising of Single Scan Raman Spectroscopy Signals. *Imaging, Manipulation, and Analysis of Biomolecules, Cells, and Tissues Viii*, 7568 (2010).

* Discussion about methods of noise reduction in images of the scanned tissues derived from Raman spectra

18. Barman I, Dingari N, Singh G, Soares J, Dasari R, Smulko J. Investigation of Noise-Induced Instabilities in Quantitative Biological Spectroscopy and Its Implications for Noninvasive Glucose Monitoring. *Analytical Chemistry*, 84(19), 8149-8156 (2012).

* Discussion of inherent noise in Raman spectra that influences nonlinear detection methods

19. van Spengen W, Roca J. On the noise limit of stress and temperature measurements with micro-Raman spectroscopy. *Journal of Raman Spectroscopy*, 44(7), 1039-1044 (2013).

20. Rana V, Canamares M, Kubic T, Leona M, Lombardi J. Surface-enhanced Raman Spectroscopy for Trace Identification of Controlled Substances: Morphine, Codeine, and Hydrocodone. *Journal of Forensic Sciences*, 56(1), 200-207 (2011).
21. Rock W, Bonn M, Parekh S. Near shot-noise limited hyperspectral stimulated Raman scattering spectroscopy using low energy lasers and a fast CMOS array. *Optics Express*, 21(13), 15113-15120 (2013).
22. McDowell E, Ren J, Yang Ch. Fundamental sensitivity limit imposed by dark 1/f noise in the low optical signal detection regime. *Optics Express*, 16(10), 6822-6832 (2008).
23. Gnyba M, Smulko J, Kwiatkowski A, Wierzba P. Portable Raman spectrometer-design rules and applications. *Bulletin of the Polish Academy of Sciences - Technical Sciences*, 59(3), 325-329 (2011).
24. Kotarski M, Smulko J. Assessment of synchronic detection at low frequencies through DSP-based board and PC sound card. *XIX IMEKO World Congress e Fundamental and Applied Metrology*, *September 6-11*, 960-963 (2009).

* Review of synchronous detection methods and measurement systems to reduce noise

25. Keller M, Vargis E, Granja N *et al.* Development of a spatially offset Raman spectroscopy probe for breast tumor surgical margin evaluation. *Journal of Biomedical Optics*, 16(7), 077006 (2011).
26. Maher J, Berger A. Determination of Ideal Offset for Spatially Offset Raman Spectroscopy. *Applied Spectroscopy*, 64(1), 61-65 (2010).
27. Kogan S. Electronic noise and fluctuations in solids. Cambridge University Press (2008).

** Comprehensive overview of noise mechanisms and noise sources in materials and sensors

28. Foster S, Cranch, GA, Tikhomirov, A. Experimental evidence for the thermal origin of 1/f frequency noise in erbium-doped fiber lasers. *Physical Review A*, 79(5), 053802-053808 (2009).
29. Poglitsch A, Waelkens C, Geis N *et al.* The photodetector array camera and spectrometer (PACS) on the Herschel space observatory. arXiv preprint arXiv:1005.1487 (2010).
30. Jiang YY, Ludlow AD, Lemke ND *et al.* Making optical atomic clocks more stable with 10-16-level laser stabilization. *Nature Photonics*, 5(3), 158-161 (2011).
31. Bell SEJ, Bourguignon E, Dennis A. Analysis of luminescent samples using subtracted shifted Raman spectroscopy. *Analyst*, 123, 1729–1734 (1998).
32. Bell SEJ, Bourguignon E, Dennis AC, Fields JA, McGarvey JJ, Seddon KR. Identification of dyes on ancient Chinese paper samples using the subtracted shifted Raman spectroscopy method. *Analytical Chemistry*, 72(1), 234-239 (2000).
33. O'Grady A, Dennis AC, Denvir D, McGarvey JJ, Bell SE. Quantitative Raman spectroscopy of highly fluorescent samples using pseudosecond derivatives and multivariate analysis. *Analytical Chemistry*, 73(9), 2058-65 (2001).
34. Dingari N, Barman I, Kang J, Kong C, Dasari R, Feld M. Wavelength selection-based nonlinear calibration for transcutaneous blood glucose sensing using Raman spectroscopy. *Journal of Biomedical Optics*, 16(8), 087009 (2011).
35. Barman I, Singh G, Dasari R, Feld M, Vaidyan V, Jayakumar V. Transcutaneous Measurement of Blood Analyte Concentration Using Raman Spectroscopy. *Perspectives in Vibrational Spectroscopy*, 1075, 33-37 (2008).
36. Kwiatkowski A, Gnyba M, Smulko J, Wierzba P. Algorithms of chemicals detection using Raman spectra. *Metrology and Measurement Systems*, 17(4), 549-559 (2010).

** Comparative analysis of various algorithms used to detect chemical compounds by Raman spectra

37. Zhang Z, Chen S, Liang Y *et al.* An intelligent background-correction algorithm for highly fluorescent samples in Raman spectroscopy. *Journal of Raman Spectroscopy*, 41(6), 659-669 (2010).
38. Praveen B, Ashok P, Mazilu M, Riches A, Herrington S, Dholakia K. Fluorescence suppression using wavelength modulated Raman spectroscopy in fiber-probe-based tissue analysis. *Journal of Biomedical Optics*, 17(7) (2012).
39. Mazilu M, De Luca A, Riches A, Herrington C, Dholakia K. Optimal algorithm for fluorescence suppression of modulated Raman spectroscopy. *Optics Express*, 18(11), 11382-11395 (2010).
40. Bonnier F; Ali SM; Knief P *et al.* Analysis of human skin tissue by Raman microspectroscopy: Dealing with the background. *Vibrational Spectroscopy* 61, 124-132 (2012).
41. Biscar JP, Kollias N, Light scattering from albumins. *Chemical Physics Letters*, 24(4), 563-564 (1974).
42. Wood BR, Hammer L, Davis L, McNaughton D, Raman microspectroscopy and imaging provides insights into heme aggregation and denaturation within human erythrocytes. *Journal of Biomedical Optics* 10(1), 014005.1-014005.13 (2005).
43. McCain S, Willett R, Brady D. Multi-excitation Raman spectroscopy technique for fluorescence rejection. *Optics Express*, 16(15), 10975-10991 (2008).
44. Cooper J, Abdelkader M, Wise K. Sequentially Shifted Excitation Raman Spectroscopy: Novel Algorithm and Instrumentation for Fluorescence-Free Raman Spectroscopy in Spectral Space. *Applied Spectroscopy*, 67(8), 973-984 (2013).
45. Mozharov S, Nordon A, Littlejohn D, Marquardt B. Automated Cosmic Spike Filter Optimized for Process Raman Spectroscopy. *Applied Spectroscopy*, 66(11), 1326-1333 (2012).
46. Nolen C, Denina G, Teweldebrhan D, Bhanu B, Balandin A. High-throughput large-area automated identification and quality control of graphene and few-layer graphene films. *ACS nano*, 5(2), 914-922 (2011).
47. Toh K, Isa N. Noise adaptive fuzzy switching median filter for salt-and-pepper noise reduction. *Signal Processing Letters, IEEE*, 17(3), 281-284 (2010).
48. Reddy RK, Bhargava R. Chemometric Methods for Biomedical Raman Spectroscopy and Imaging. In Emerging Raman Applications and Techniques in Biomedical and Pharmaceutical Fields. Springer Berlin Heidelberg 179-213 (2010).
49. Jolliffe I. Principal component analysis. John Wiley & Sons, Ltd (2005).
50. Bodanese B, Silveira L, Albertini R, Zângaro RA, Pacheco MTT. Differentiating normal and basal cell carcinoma human skin tissues in vitro using dispersive Raman spectroscopy: a comparison between principal components analysis and simplified biochemical models. *Photomedicine and Laser Surgery*, 28(S1), 119-127 (2010).
51. Barman I, Dingari N, Rajaram N, Tunnell J, Dasari R, Feld M. Rapid and accurate determination of tissue optical properties using least-squares support vector machines. *Biomedical Optics Express*, 2(3), 592-599 (2011).
52. Feng S, Chen R, Lin J *et al.* Nasopharyngeal cancer detection based on blood plasma surface-enhanced Raman spectroscopy and multivariate analysis. *Biosensors and Bioelectronics*, 25(11), 2414-2419 (2010).
53. Dingari N, Barman I, Saha A *et al.* Development and comparative assessment of Raman spectroscopic classification algorithms for lesion discrimination in stereotactic breast biopsies with microcalcifications. *Journal of Biophotonics*, 6(4), 371-381 (2013).
54. Bergholt M, Zheng W, Lin K *et al.* Characterizing variability in in vivo Raman spectra of different anatomical locations in the upper gastrointestinal tract toward cancer detection. *Journal of*

Biomedical Optics, 16(3), 037003 (2011).
55. Lui H, Zhao J, McLean D, Zeng H. Real-time Raman spectroscopy for in vivo skin cancer diagnosis. *Cancer research*, 72(10), 2491-2500 (2012).

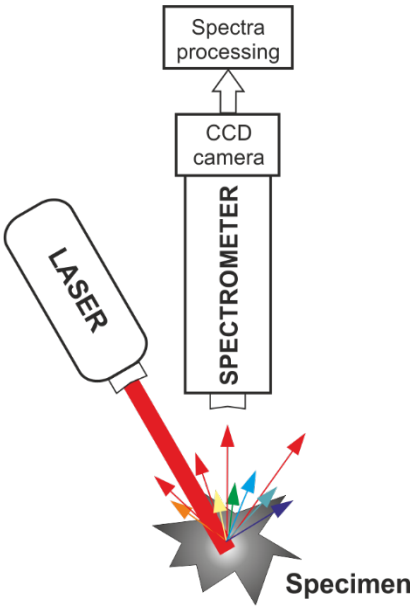

Figure 1. A schematic diagram of Raman spectroscopy setup and spectra processing

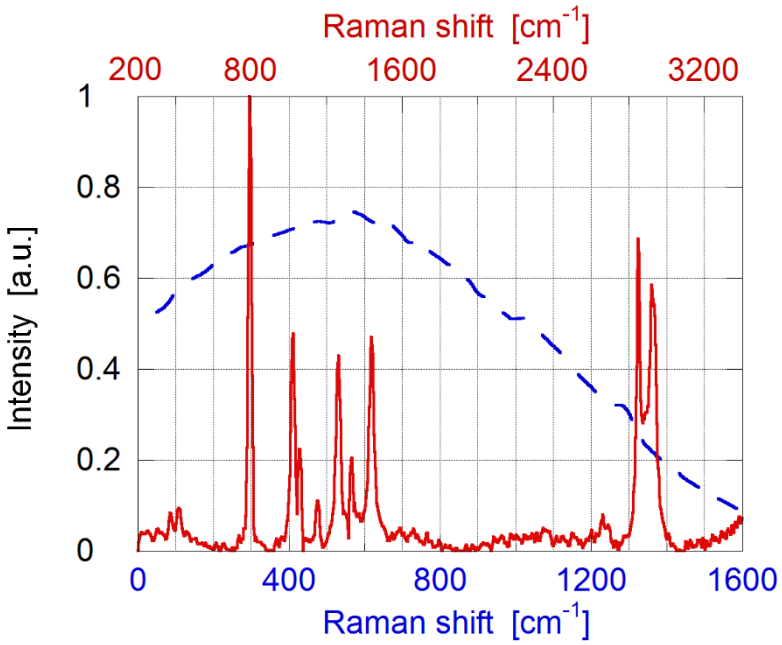

Figure 2. Representative Raman spectra of cyclo-hexane (red continuous line) and skin tissue (blue dashed line) acquired to identify blood glucose level [18]. Despite the large Raman scattering cross-section of the cyclo-hexane molecule, the endogenous tissue autofluorescence (broad background in the blue dashed line) is still significantly larger. Clearly, this is an even bigger problem for quantitation of molecules with moderate Raman scattering cross-sections and that have less concentration in the biological sample of interest.

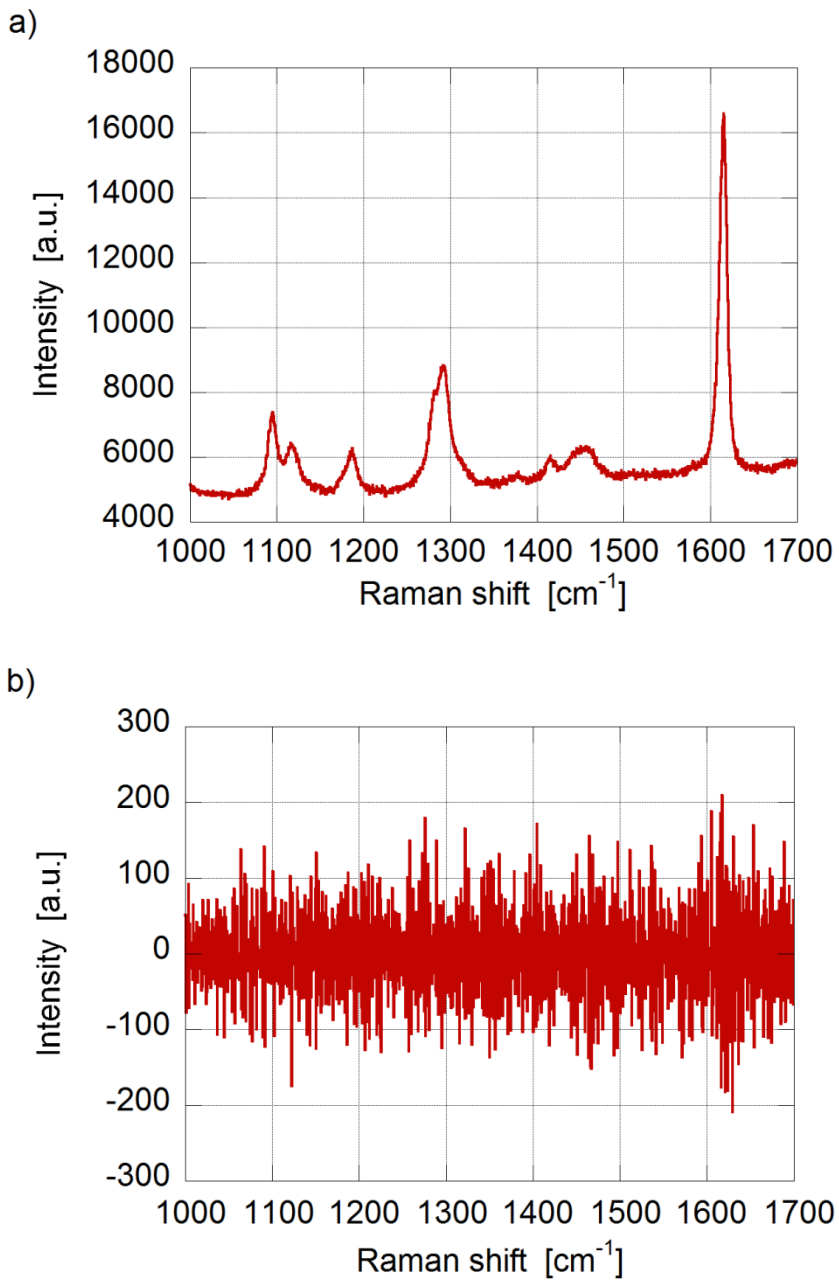

Figure 3. A fragment of: a) the acquired Raman spectrum and b) its noise component non-uniformly distributed versus Raman shift

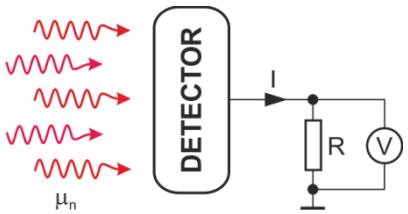

Figure 4. Schematic of the sensor detecting photons by measuring voltage drop across the resistance *R* induced by electron current *I*

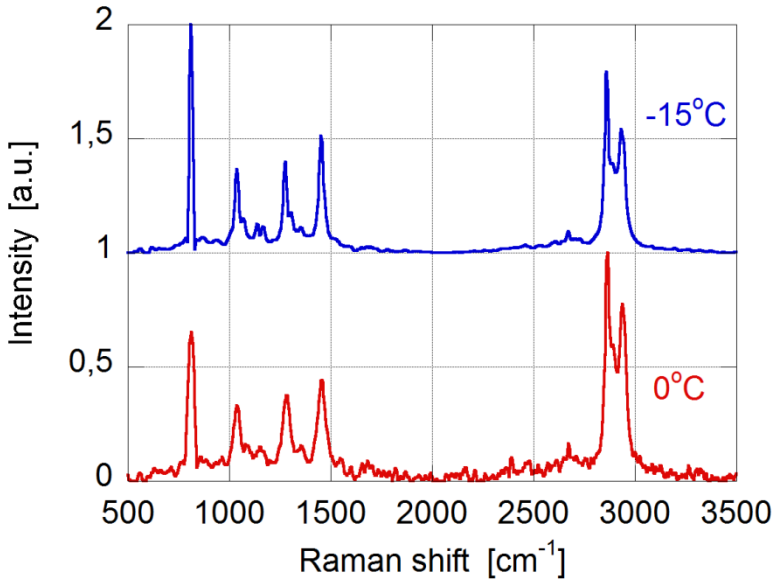

Figure 5. Raman spectrum of a representative chemical specimen measured at the same acquisition time but at two different temperatures of the CCD sensor: 0°C (red line), -15°C (blue line)

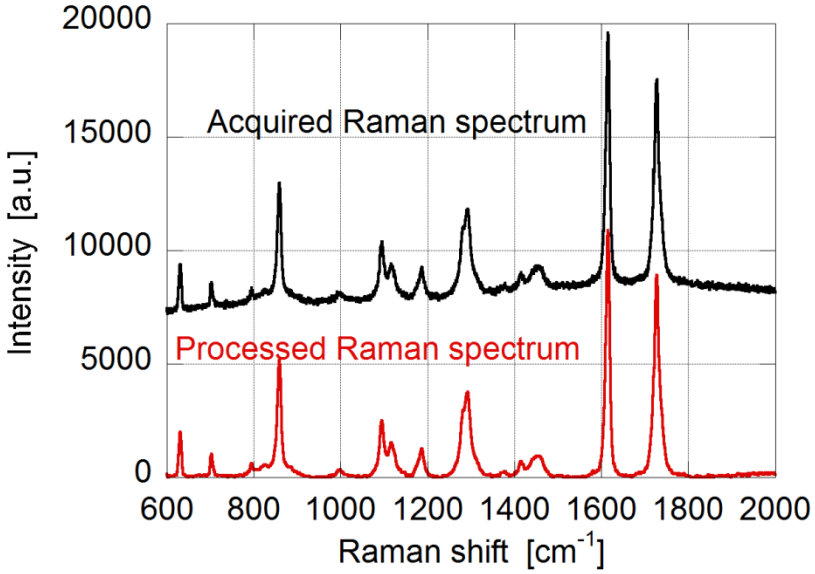

Figure 6. Efficiency of processing the acquired Raman spectrum (black line) by smoothing and background removal (red line) using Savitzky-Golay filtering for smoothing and polynomial approximation for background removal